

*2007 ECI Conference on The 12th International Conference on
Fluidization - New Horizons in Fluidization Engineering*

Vancouver, Canada

Editors: Franco Berruti, The University of Western Ontario, London,
Canada

Xiaotao (Tony) Bi, The University of British Columbia, Vancouver, Canada

Todd Pugsley, University of Saskatchewan, Saskatoon, Saskatchewan,
Canada

Year 2007

Paper 39

Dynamic Simulation of Gas Hydrate
Formation in an Agitated Three-Phase Slurry
Reactor

Shahrzad Hashemi* Arturo Macchi †
Phillip Servio‡

*University of Ottawa

†University of Ottawa

‡McGill University

http://services.bepress.com/eci/fluidization_xii/39

Copyright ©2007 by the authors.

Dynamic Simulation of Gas Hydrate Formation in an Agitated Three-Phase Slurry Reactor

Abstract

Gas hydrate growth was simulated in an agitated three-phase slurry reactor using a dynamic model that incorporates hydrate formation kinetics as well as system hydrodynamics and interphase heat and mass transfer rates. Supersaturation ratios and mole consumption rates were evaluated as a function of time for different gas and liquid superficial velocities. Based on available data and the conditions investigated, the kinetic resistance was found to be more influential than the resistance to gas-liquid mass transfer.

Dynamic Simulation of Gas Hydrate Formation in an Agitated Three-Phase Slurry Reactor

Shahrzad Hashemi, Arturo Macchi*

*Department of Chemical Engineering, University of Ottawa, Ottawa, Ontario, Canada, K1N 6N5, *F: 1-613-562-5172; E: macchi@eng.uottawa.ca*

Phillip Servio

Department of Chemical Engineering, McGill University, Montreal, Quebec, Canada, H3A 2B2

ABSTRACT

Gas hydrate growth was simulated in an agitated three-phase slurry reactor using a dynamic model that incorporates hydrate formation kinetics as well as system hydrodynamics and interphase heat and mass transfer rates. Supersaturation ratios and mole consumption rates were evaluated as a function of time for different gas and liquid superficial velocities. Based on available data and the conditions investigated, the kinetic resistance was found to be more influential than the resistance to gas-liquid mass transfer.

INTRODUCTION

Gas hydrates are non-stoichiometric crystalline compounds that form when a single gas or volatile liquid molecule occupies the cages of structured water (1). Hydrate compounds, containing mostly methane, are made naturally within the permafrost zone and in sub-sea sediment at temperature and pressure conditions within the thermodynamic stability region (1). Methane hydrate is considered a potential energy resource due to its immense quantities and wide geographical distribution. Synthesis of gas hydrates is regarded as a means to capture carbon dioxide from flue gases as well as an alternate method of transportation and storage of natural gas as they eliminate the necessity of very low temperatures (-160 °C for Liquefied Natural Gas, LNG) and very high pressures (200 atm for Compressed Natural Gas, CNG). The hydrate contains about 160 Sm³ per m³ of hydrate, which is comparable to LNG and CNG, at near ambient temperatures (0 to -10 °C) and pressures (10 to 1 atm) (2).

The various multiphase systems that have been suggested to produce gas hydrate can be categorized into two groups such that liquid (3) or gas (4) is the dispersed phase. The latter is preferred over the former as gas-liquid mass transfer can be improved by bubbling the gas into the liquid phase. In addition, systems with liquid as the continuous phase benefit from the greater heat capacity of water in order to remove the heat produced from hydrate formation. In this work, a dynamic model that depicts CO₂ hydrate formation in an agitated slurry reactor is presented.

MODEL DEVELOPMENT

The hydrate growth system is represented by gas bubbles and growing hydrate particles dispersed in liquid water. Initially gas is dissolved into the liquid in order to create a supersaturated solution. Then, at a specific time called the turbidity point, nucleation occurs generating the seed hydrate particles. Afterwards, by ensuring low supersaturation conditions, gas consumed is assumed to be utilized for growth of already formed hydrates rather than for nucleation. Thus, gas molecules transfer from the bubbles to the gas-liquid interface, then diffuse through the liquid film to the bulk and finally incorporate onto the surface of hydrate particles. Gas and liquid phases are assumed to be at equilibrium at the interface where the concentration is evaluated at the temperature and pressure of the system (5). For sparingly soluble gases, the gas-liquid mass transfer resistance is restricted within the liquid film.

Based on the theory of crystallization (6), gas is adsorbed onto the surface of hydrate crystals in two consecutive steps. Gas molecules first diffuse through the liquid film surrounding the crystal towards the surface where they are then adsorbed onto the surface of the crystal due to the lower energy provided at the surface. The enclathration of gas onto the surface is controlled by the equilibrium concentration, which is the solubility of the gas hydrate former in water at the crystal surface temperature (7) and system pressure as it is uniform among all phases (1). Equilibrium concentrations at the gas-liquid and hydrate-liquid interfaces were estimated using the model proposed by Hashemi et al. (8). There is no concentration or temperature gradient across the crystal. Moreover, temperature differences across the liquid films at the gas-liquid and hydrate-liquid interfaces due to respectively the heat of dissolution and hydrate formation were found to be negligible (7). Figure 1 summarizes the pressure, temperature and concentration gradients across the different phases.

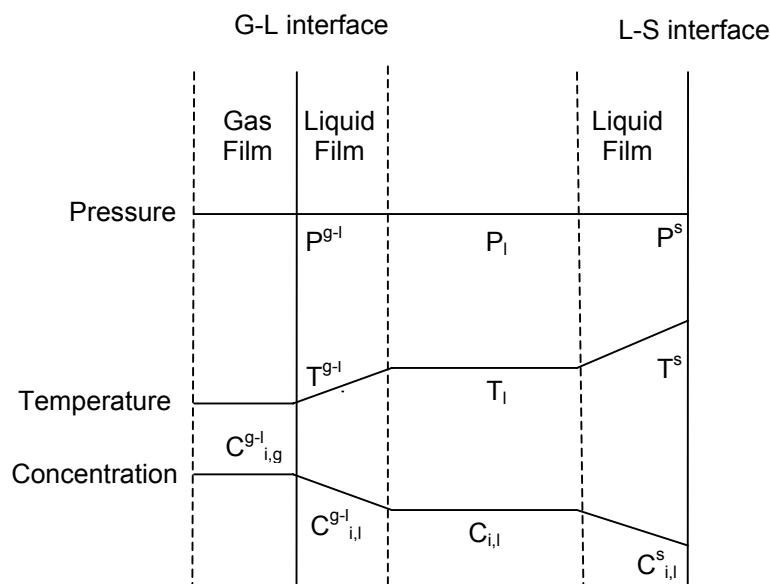


Figure 1- Temperature, pressure and concentration driving forces within the gas, liquid and solid phases

The mass balance of component i in the gas, liquid and solid phases for the reactor presented in figure 2 is given by equations (1) to (3). It is assumed that the rate of mass transfer in the liquid film layers is low and there is no accumulation of gas at the gas-liquid and hydrate-liquid interfaces. Water is in excess and is assumed not to limit the rate of hydrate formation.

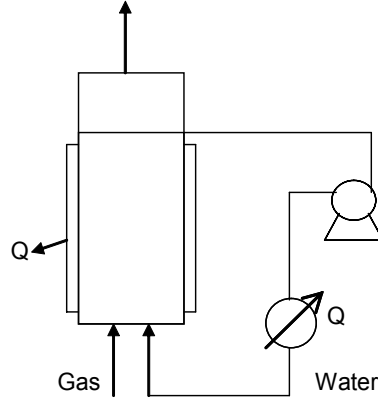


Figure 2- Schematic of the experimental apparatus

$$C_{i,g}(U_g)_{in}A - C_{i,g}(U_g)_{out}A - k_l a_l \varepsilon_l (C_{i,l}^{g-l} - C_{i,l})V_R = V_R \frac{d(C_{i,g}\varepsilon_g)}{dt} \quad (1)$$

$$(C_{i,l}U_l)_{in}A - (C_{i,l}U_l)_{out}A + k_l a_l \varepsilon_l (C_{i,l}^{g-l} - C_{i,l})V_R - k_s a_s (C_{i,l} - C_{i,l}^s)V_R = V_R \frac{d(C_{i,l}\varepsilon_l)}{dt} \quad (2)$$

$$k_s a_s (C_{i,l} - C_{i,l}^s)V_R = k_r a_s (C_{i,l}^s - C_{i,l}^{eq})V_R \quad (3)$$

where

$$\varepsilon_l + \varepsilon_g + \varepsilon_s = 1 \quad (4)$$

The concentration of gas molecules at the solid surface $C_{i,l}^s$ can be eliminated by combining the two terms in eq. (3) and introducing a combined mass transfer and kinetic resistance around the solid hydrate particles ($1/K^*$):

$$\frac{1}{K^*} = \frac{1}{k_r} + \frac{1}{k_s} \quad (5)$$

Since there is negligible change in the molar flow rate of dissolved component i in the liquid return line, the first two terms on the left side of eq. (2) are considered equal and eq. (2) can be rewritten as:

332

HASHEMI, MACCHI, SERVIO

$$k_l a_l \varepsilon_l (C_{i,l}^{g-l} - C_{i,l}) V_R - K^* a_s (C_{i,l} - C_{i,l}^{eq.}) V_R = V_R \frac{d(C_{i,l} \varepsilon_l)}{dt} \quad (6)$$

The particle surface area a_s and the solid holdup ε_s per unit volume of reactor can be obtained from the second and third moment of a population balance (9) assuming that there is no particle breakage or agglomeration in the system:

$$\frac{d\mu_j}{dt} = jG\mu_{j-1} \quad \mu_j(0) = \mu_j^0, j = 0, 1, 2, 3 \quad (7)$$

Where a_s and ε_s are respectively $\pi\mu_2$ and $\pi\mu_3/6$ assuming spherical particles. G is the linear growth rate expressed by the following equation:

$$G = \frac{K^* M_H (C_{i,l} - C_{i,l}^{eq.})}{\rho_H} \quad (8)$$

The number of particles per unit volume of reactor μ_0 at the turbidity point can be calculated by the excess gas converted to hydrate nuclei as follows:

$$\mu_0^0 = \frac{N_p}{V_R} = \frac{3M_H (n_{tb} - n_{eq})}{4\pi V_R \rho_H r_{cr}^3} \quad (9)$$

The initial conditions for the first, second and third moments are (9):

$$\mu_j^0 = 2^j (r_{cr})^j \mu_0^0 \quad j = 1, 2, 3 \quad (10)$$

The initial size of particles can also be found from the following equation (9):

$$r_{cr} = \frac{-2\sigma}{\Delta g} \quad (11)$$

where

$$-\Delta g = \frac{RT_{exp}}{v_H} \left(\ln \frac{f_{tb}(T_{exp}, P_{exp}, X_{tb})}{f_{eq}(T_{exp}, P_{exp}, X_{eq})} + n_w \ln \frac{f_{w,tb}(T_{exp}, P_{exp}, (1 - X_{tb}))}{f_{w,eq}(T_{exp}, P_{exp}, (1 - X_{eq}))} \right) \quad (12)$$

Here X_{tb} and X_{eq} are the gas hydrate former mole fraction at the turbidity point and hydrate-liquid water equilibrium, respectively. The number of moles dissolved in the liquid at the turbidity point is assumed equal to that at vapor-liquid equilibrium.

Gas holdup ε_g and the volumetric liquid-side mass transfer coefficient $k_l a_l$ were estimated by the correlations developed by Behkish et al. (10) and Lau et al. (11),

respectively. The liquid-solid convective mass transfer coefficient k_s is estimated by the following equation (12):

$$Sh = 2 + 0.4 Re^{0.25} Sc^{1/3} \quad (13)$$

Gas diffusivity was estimated using the equations proposed by Wilke and Chang (13). Hydrate physical parameters were obtained from the work of Malegaonkar et al. (14) while the intrinsic kinetic rate constant was taken from the theoretical results of Hashemi et al. (7).

RESULT AND DISCUSSION

Figure 3 shows the bulk supersaturation ratio C_l / C_{eq} of carbon dioxide in water as a function of time at 277.15 K, 21.87 bar and a liquid velocity of 0.002 m/s. Gas and liquid inlet temperatures were kept at 275.15 K. The simulation was not continued for a time period beyond 10 minutes as the probability of particles forming agglomerates or large particles breaking due to particle-particle, particle-stirrer and particle-wall collisions would be even greater (9). In order to take these phenomena into account, the particle size distribution needs to be measured in situ.

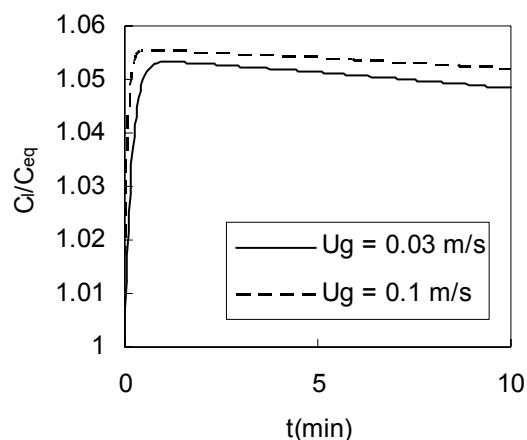


Figure 3- Supersaturation ratio of carbon dioxide in water as a function of time at 277.15 K and 21.87 bar; liquid velocity is 0.002 m/s.

Time equal to zero corresponds to the turbidity point where no more particles are generated by nucleation. The liquid-solid mass transfer resistance ($1/k_s$) was found insignificant relative to the kinetic resistance ($1/k_r$) with the former 10^7 times smaller than the latter. It was found that the supersaturation ratio decreased by only 0.1% when neglecting the change in liquid holdup with time, see eq. (6), while the curves maintained the same trend. It was assumed that at the onset of turbidity, the gas hydrate former concentration drops to the two-phase liquid-hydrate equilibrium value. This leads to a high gas dissolution driving force as $(C_l^{g-l} - C_l)$ is larger than $(C_l - C_l^{eq})$ resulting in the accumulation of gas in the liquid bulk. The increase in the bulk concentration proceeds to a point where the rate of gas dissolution is equal to the rate of gas hydrate formation. Afterwards, the consistent increase in solid area results in a decrease in the bulk concentration, see eq. (6), and hence a lower driving force, see eq. (8), which in turn impedes the particles growth, see eq. (7) for j

= 2. The rate of gas dissolution remains almost equal to the rate of gas hydrate formation as the supersaturation ratio decreases with a slope lower than -0.01 s^{-1} . The mole consumption rate slowly increases during this time with a maximum (at 10 minutes) of 0.0068 and 0.0076 mol/s at gas velocities of 0.03 and 0.1 m/s, respectively. The amount of heat to be removed also slowly increases during this time with a maximum of 0.73 and 0.85 KJ/s at gas velocities of respectively 0.03 and 0.1 m/s. Considering the system as quasi steady-state, the kinetic resistance ($1/k_l a_s$) was found to be more influential than the gas-liquid mass transfer resistance ($1/k_l a_l \epsilon_l$) with the effect naturally more pronounced at higher gas velocities resulting in greater supersaturation ratios. The supersaturation ratio increases with an increase in liquid velocity although the effect is less noticeable than that of gas velocity since $k_l a_l$ is more sensitive to the gas than the liquid velocity.

The technology for large-scale synthesis of gas hydrates is still in the conceptual mode and there is almost no data available in the open literature. To the authors' knowledge, the only published data for a similar system to this work is from Mork and Gudmundsson (4) who produced methane hydrates. They reported an apparently constant mole consumption rate suggesting that the hydrate formation rate is strongly controlled by interphase mass transfer rather than kinetics. In their case, they were mechanically limited to relatively low gas superficial velocities below 0.002 m/s. More work is required to improve the accuracy of the available intrinsic kinetic rate data as well as to obtain hydrodynamic data in a pilot scale system at hydrate forming operating conditions. We are in the commissioning stages of a reactor of 0.1 m in diameter capable of sustaining pressures up to 10 MPa. The gas and liquid velocities can be varied up to 0.40 and 0.10 m/s, respectively. As in figure 2, the reactor wall is jacketed and there is an external shell and tube heat exchanger for additional removal of heat of hydrate formation. Experiments in this system should provide useful data to test the accuracy of the proposed model and provide information for the design of this novel technology for gas capture and storage.

CONCLUSION

A dynamic gas hydrate growth model was formulated for an agitated three-phase slurry reactor. The model uses a theoretical population balance and is based on driving forces that require estimates of gas-liquid and liquid-hydrate equilibrium concentrations. For the range of operating conditions investigated, mole consumption rates were affected more by hydrate formation kinetics than by gas-liquid mass transfer. However, at present, there is insufficient available experimental data to validate the proposed model. More work is required to obtain accurate intrinsic kinetic rate constants as well as transport properties at hydrate forming conditions.

NOTATION

a_s	liquid-solid interfacial area per unit volume of reactor, $\text{m}_{\text{hyd.}}^2 \text{ m}_R^{-3}$
A	cross sectional area of reactor, m^2
C	concentration, mol m^{-3}
d_p	particle diameter, μ_1 / μ_0 , m
D	diffusivity in liquid, $\text{m}^2 \text{ s}^{-1}$

f	fugacity, Pa
G	linear growth rate, m s^{-1}
k_r	intrinsic kinetic rate constant, $\text{m}_{\text{liq.}}^3 \text{m}_{\text{hyd.}}^{-2} \text{s}^{-1}$
$k_l a_l$	volumetric liquid-side mass transfer coefficient, s^{-1}
k_s	liquid-solid convective mass transfer coefficient, $\text{m}_{\text{liq.}}^3 \text{m}_{\text{hyd.}}^{-2} \text{s}^{-1}$
K^*	combined rate parameter, $\text{m}_{\text{liq.}}^3 \text{m}_{\text{hyd.}}^{-2} \text{s}^{-1}$
M	molecular weight of the hydrate of the form $\text{CO}_2 \cdot n_w \text{H}_2\text{O}$
N_p	number of particles in the liquid phase
n	moles of gas consumed, mol
Q	rate of heat removal, KJ s^{-1}
R	gas constant, $\text{J mol}^{-1} \text{K}^{-1}$
Re	$(U_g g d_p^4 / \nu_l)^{1/3}$
P	pressure, Pa
r_{cr}	critical radius, m
Sh	$k_s d_p / D$
Sc	$\mu_l / \rho_l D$
T	temperature, K
t	time, s
U	velocity, m s^{-1}
V_R	reactor volume, m^3
v	molar volume, $\text{m}^3 \text{mol}^{-1}$
X	mole fraction

Greek letters

ε	phase holdup
ρ	density, kg m^{-3}
σ	surface tension for a hydrate-water system, J m^{-2}
Δg	free energy change per unit volume of product, J m^{-3}
ν	kinematic viscosity, $\text{m}^2 \text{s}^{-1}$
μ	viscosity, Pa s
μ_j	n-th moment of particle distribution, $\text{m}^j \text{m}_R^{-3}$
μ_j^0	initial n-th moment of particle distribution

Subscripts and Superscripts

i	gas component
$eq.$	hydrate-liquid water equilibrium
exp	experimental condition
g	gas phase
$g-l$	gas-liquid interface
H	hydrate phase

336

HASHEMI, MACCHI, SERVIO

<i>l</i>	liquid bulk
<i>s</i>	surface of solid, solid(hydrate) phase
<i>tb</i>	turbidity point
<i>w</i>	water

ACKNOWLEDGMENTS

The authors are grateful to the Natural Sciences and Engineering Research Council of Canada for financial assistance.

REFERENCES

- [1] Sloan, Jr. E.D., (1998). Clathrate Hydrates of natural gases. 2nd ed. New York: Marcel Dekker.
- [2] Thomas, S., Dawe, R.A., (2003). Review of ways to transport natural gas energy from countries which do not need the gas for domestic use. *Energy*, 28, 1461-1477.
- [3] Iwasaki, S., Kimura T., Yoshikawa K., Nagayasu H., (2002). The pre-investigation of natural gas transportation and storage system as gas hydrates for development of marginal natural gas fields. Proceeding of the 4th International Conference on Gas Hydrates, Yokohama.
- [4] Mork, M., Gudmundsson, J.S., (2002). Hydrate formation rate in a continuous stirred tank reactor: Experimental results and Bubble-to-Crystal model. Proceeding of the 4th International Conference on Gas Hydrates, Yokohama.
- [5] Herri, J.M., Pic, J.S., Gruy, F., Cournil, M., (1999). Methane hydrate crystallization mechanism from in-situ particle sizing. *A.I.Ch.E Journal*, 45, 590-602.
- [6] Mullin, J.W., (1992). Crystallization. 3rd ed. Butterworth Heinemann.
- [7] Hashemi, S., Macchi, A., Servio, P. Hydrate growth model in a semi-batch stirred tank reactor. submitted to *Ind. Eng. Chem. Res.*
- [8] Hashemi, S., Macchi, A., Bergeron S., Servio, P. (2006). Prediction of methane and carbon dioxide solubility in water in the presence of hydrate. *Fluid Phase Equilibria*, 246, 131-136.
- [9] Englezos, P., Kalogerakis, N., Dholabhai, P.D., Bishnoi, P.R., (1987). Kinetics of formation of methane and ethane gas hydrates. *Chemical Engineering Science*, 42, 2647-2658.
- [10] Behkish, A., Lemoine, R., Oukaci, R., Morsi, B.I., (2006). Novel correlations for gas holdup in large-scale slurry bubble column reactors operating under elevated pressures and temperatures. *Chemical Engineering Journal*, 115, 157-171.
- [11] Lau R., Peng W., Velazquez-Vargas L.G., Yang G.Q., Fan L.-S., (2004). Gas-liquid mass transfer in high pressure bubble columns. *Industrial and Engineering Chemistry Research*, 43, 1302-1311.
- [12] Beenackers, A.A.C.M., Van Swaaij, W.P.M., (1993). Mass transfer in gas-liquid slurry reactors. *Chemical Engineering Science*, 48, 3109-3139.
- [13] Wilke, C.R., and Chang P., (1955). Correlation of diffusion coefficients in dilute solutions. *A.I.Ch.E Journal*, 1, 264-270.
- [14] Malegaonkar, M.B., Dholabhai, P.D., Bishnoi, P.R., (1997). Kinetics of carbon dioxide and methane hydrate formation. *Can. J. of Chem. Eng.*, 75, 1090-1099.